FLOW AROUND A 2D-CYLINDER: INFLUENCE OF BLUFF-BODIES IN THE WAKE

Robert MITRUȚ[1], Diana Maria BUCUR[2]*, Georgiana DUNCA[3], Michel J. CERVANTES[4]

The current paper presents the linear stability analysis (LSA) applied on the flow around a 2D bluff-body of circular shape at Reynolds number of 80. The LSA is applied to study the evolution of a small perturbation inserted into the flow. The spatial structures of the most unstable eigenmode are used to compute the wavemaker, i.e., the location that is the most responsive to an external force, which can act to modify the stability of the flow. Additional bluff-bodies are inserted among the main circular bluff-body in the designated zone to modify the flow dynamics and observe their shape and size influence on the flow stability.

Keywords: linear global stability analysis, sensitivity analysis, vortex shedding.

1. Introduction

During the last decades, preservation and protection of the environment became a top priority among governmental agendas. The energy sector had to develop more environmental-friendly strategies to limit the production capacity of polluting factories, encourage the use of green energy sources, etc. [1]. Despite the large amount of research, only a few green, renewable energy sources, namely wind and solar, managed to prove a high capacity of production. However, these sources present an intermittent character that affects the stability of the power grid. In this context hydropower is nowadays used to assure a proper balance between market demand and supply due to its fast response time. This backup capacity involves using the hydraulic turbines in conditions far from best efficiency point (BEP) which leads to vibrations, efficiency decrease and, in the long term, machinery and even structure fatigue under part load operations [2]. All these unwanted

[1] PhD Student, Dept. of Hydraulics, Hydraulic Machinery and Environmental Engineering, National University of Science and Technology POLITEHNICA Bucharest, Romania, e-mail: robert.mitrut@upb.ro

[2]* Professor, Dept. of Hydraulics, Hydraulic Machinery and Environmental Engineering, National University of Science and Technology POLITEHNICA Bucharest, Romania, e-mail: diana.bucur@upb.ro (corresponding author)

[3] Assoc. Professor, Dept. of Hydraulics, Hydraulic Machinery and Environmental Engineering, National University of Science and Technology POLITEHNICA Bucharest, Romania, e-mail: georgiana.dunca@upb.ro

[4] Professor, Division of Fluid and Experimental Mechanics, Luleå University of Technology, Sweden, e-mail: michel.cervantes@ltu.se

phenomena are the result of a detrimental flow structure, vortex breakdown (VB), which develops in the draft tube due to the loss of flow stability [3]. It is useful to develop numerical methods and mitigation strategies using simplified test cases [4], [5], because of the geometry and flow complexity in hydraulic turbines where VB appears.

The VB phenomenon was first studied by Peckham and Atkinson considering the air flow over a delta wing [6]. Using an experimental setup formed of a pipe with a diverging section and a bell-mouth shaped inlet including guide vanes, T. Sarpkaya reproduced different types of VB using water as flow fluid. He concluded that the VB type is influenced by the swirl number, defined as the circumferential momentum divided by the axial momentum, and the Reynolds number [7]. Wang and Rusak defined a critical swirl number which can be obtained by approaching an eigenvalue problem and corresponds to the exchange of stability point [8]. They concluded that the VB breakdown is due to the stability loss of the swirling flow. M. Kurosaka et. al reproduced different VB types using a similar apparatus to the one used by T. Sarpkaya but having a straight pipe. They also obtained different types of VB by imposing external disturbances to the flow [3]. Experimental methods were applied on simplified geometries of draft tubes to decrease the residual swirls such as air injection and stabilizer fins mounted on the walls [9], [10]. Resiga et. al successfully mitigated the pressure fluctuations using a water jet injected through the runner hub and used a mathematical model to compute the axial and tangential velocity profile which may be used in early optimization stages [11], [12].

Moreover, the flow through the turbines can be attributed to the open flow class, where the fluid particles are in a state of constant entry and exit of the experimental domain [2]. M. Kurosaka et. al and O. Reynolds remarked that this type of flows is constantly subject to infinitesimal external perturbations which in certain conditions can destabilize the flow [3], [13].

The evolution of an external infinitesimal disturbance that enters a system found in an equilibrium state can be analyzed in two manners, using a local LSA or a global LSA. The local LSA is suitable for weak non-parallel flows, i.e., the flow direction remains constant along the length of the flow domain. This approach requires a modest computing effort as it partitions the physical domain to evaluate its stability. The global LSA is suitable for strongly nonparallel flows, with the key assumption that the basic state is a truly parallel flow [14]. This assumption was extended to unsteady, i.e., time dependent, laminar flow by using the time averaged flow, i.e., the mean flow. This approach was successfully used in applications such as two-dimensional vortex shedding in the bluff bodies of circular shape wake or three-dimensional spiral vortex breakdown flows [15], [16].

An extended work to the stability analysis, namely the sensitivity analysis has recently been used to localize the flow regions most receptive to an external

force. Therefore, the flow properties corresponding to stability can be modified by a small perturbation applied to the main flow such as physical object, boundary conditions, advection rate or localized forces more efficiently. Experimental and numerical work has been carried out in order to determine the effect of a small control body of cylindric shape behind the main bluff body. It was shown that a suitably placed control cylinder may decrease the vortex shedding frequency [17]. Giannetti and Luchini [18] and O. Marquet [19] developed a systematic approach to diminish this frequency using a local force proportional to the disturbance amplitude, representing a source in the stability equations.

In the present paper, numerical simulations of an incompressible laminar flow around bluff-body of circular shape are performed at Re = 80. The flow dynamics are analyzed from both steady and unsteady state solutions. The steady state solution is found solving dimensionless Navier-Stokes equations in a time-independent manner, i.e., the term containing the partial derivative in respect with time is removed. The steady flow solution is used for initialization of the unsteady flow simulation to assure a faster convergence of the results. The mean flow, i.e., time averaged flow extracted from the unsteady solution and the steady flow solutions are further used to perform the stability analysis. The obtained results provide relevant information to develop techniques (active and passive) to control and manipulate the flow more effectively [20].

2. Problem formulation

The dynamics of an incompressible laminar unsteady flow is described by the following dimensionless Navier-Stokes equations:

$$\begin{cases} \partial U/\partial t + U \cdot \nabla U = -\nabla p + \mathrm{Re}^{-1} \nabla^2 U \\ \nabla \cdot U = 0 \end{cases} \tag{1}$$

where $U=(u,v,w)$ is the velocity field, Re is the Reynolds number and p is the pressure. To obtain the dimensionless form of equations (1), for the length, velocity, and pressure are used as reference the diameter of the 2D-cylinder, D, the flow velocity U_∞ and the density of the fluid.

In the linear stability theory, the total field is obtained by summing the base flow and a small perturbation:

$$U = U_b + \varepsilon U'; \; p = p_b + \varepsilon p' \tag{2}$$

where $U'=(u',v',w')$ and p' are the perturbation terms while $\varepsilon \ll 1$ denotes an infinitesimal magnitude. The linearized Navier-Stokes equations are determined by introducing the equations (2) into (1):

$$\begin{cases} \partial U'/\partial t + U_b \cdot \nabla U' + U' \cdot \nabla U_b = -\nabla p' + \mathrm{Re}^{-1} \nabla^2 U' \\ \nabla \cdot U' = 0 \end{cases} \tag{3}$$

The investigation procedure of a perturbation behavior, based on the set of equations (3) and considering that the perturbation can be decomposed into a spatial structure that grows or decays exponentially in space and time, is presented in detail in [21].

To identify the location where the instabilities arise, the following quantity is determined:

$$S = \frac{\overline{q} \otimes \overline{q}^*}{\langle \overline{q}, \overline{q}^* \rangle} \tag{4}$$

where $\overline{q}$ and $\overline{q}^*$ represent the spatial structure, also known as the direct field, and the adjoint field.

This location, referred to as a *wavemaker*, could be used to introduce a small control bluff-body to modify the flow structure and damp the instabilities [18], [19], [22].

3. Geometry and boundary conditions

The geometry used in the current research consists of a 2D rectangular domain containing a 2D cylinder, as shown in Fig. 1. The diameter is $D = 1$. The bluff-body is placed at $40D$ downstream of the domain's inlet and at $80D$ upstream the outlet. The width of the domain is $80D$.

The cartesian system origin is set at the circular shape center, at $(x, y) = (0, 0)$. The x-axis corresponds to the main flow direction (streamwise), while the y-axis is perpendicular to x-axis.

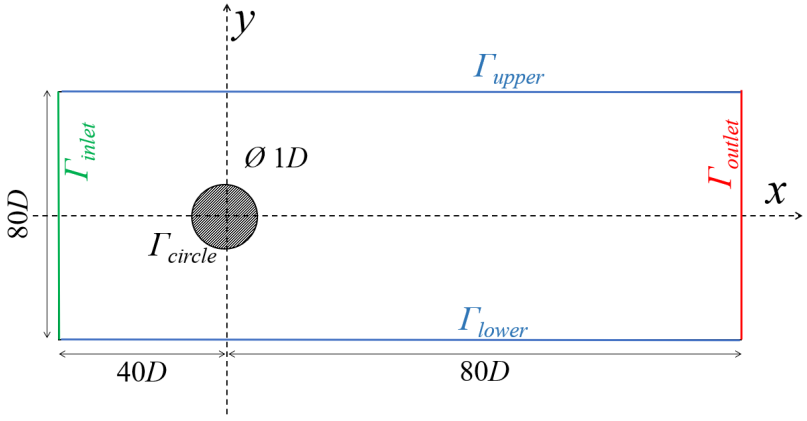

Fig. 1. Computational domain geometry

To compute the base flow, a value of 1 is set for the dimensionless velocity $U_\infty = 1$ on the inlet of the domain Γ_{inlet}, i.e., $(u, v) = (1, 0)$. A free-outlet boundary condition is set, Γ_{outlet}. The bluff-body is considered fixed with *no-slip* wall

boundary condition, $(u,v)=(0,0)$ on Γ_{circle}. To avoid any confinement effects which could affect the flow around the bluff-body, the upper and lower limits of the domain, Γ_{upper} and Γ_{lower} are set as *slip walls*, $\partial u/\partial y=0; v=0$.

For the eigenvalue problem, the perturbation terms are set to a null value on the inlet and wall, i.e., $\overline{u}=\overline{v}=\overline{w}=0$ on Γ_{inlet} and Γ_{circle}.

The analyzing domain is discretized using the AdaptMesh procedure available through FreeFEM++. When conducting numerical simulations, the mesh has a crucial aspect in providing relevant results. However, a consensus should be reached between mesh quality and dimensions reported to the results and computational time. A mesh too coarse could lead to a low computational time at the cost of unrealistic results while on the other hand, a mesh too fine could provide good results at the cost of an increased computational time. In the present research, the interest zone is in the bluff-body wake where small vortices shed periodically after a certain time. Thus, the mesh is adapted to the Hessian of the streamwise velocity resulting in a refined discretization following the vortex shedding path as it is shown in Fig. 2:

$$D^2u=(\partial^2u/\partial x^2,\partial^2u/\partial x\partial y,\partial^2u/\partial y^2) \tag{5}$$

The entire procedure is detailed in [21].

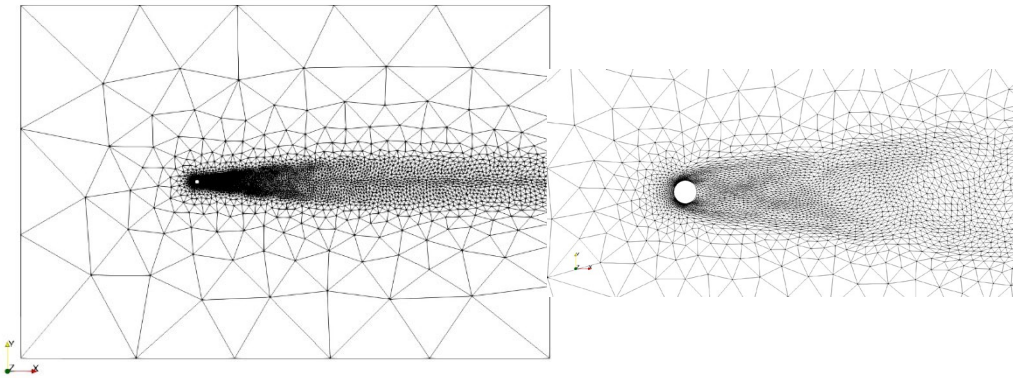

Fig. 2. Spatial discretization of the computational domain using tetrahedral elements: left – entire domain, right – close-up detail [21]

4. Results and discussions

A monitoring point is used to acquire the streamwise velocity at each iteration to extract relevant information about the vortex shedding occurrence. The mean flow is determined by time-averaging the flow over a period of 20 fully cycles of developed vortex shedding.

The global LSA is carried on the steady and mean flow fields to observe the evolution and the onset of the infinitesimal disturbances. Further, several bluff-bodies of circular and elliptical shapes are physically modelled into the domain with the purpose of decreasing the disturbances growth rate and stabilizing the flow.

In the following, the steady and unsteady flow solutions as well as comparison with the available data in the literature are presented. The section dedicated to the global LSA is divided into four subparagraphs. First and second subparagraphs presents the spatial structures of the most unstable eigenmodes (direct and adjoint) related to the leading eigenvalues. The third subparagraph shows the wavemaker region, i.e., the most receptive zones to a base flow modification. Finally, the influence of circular and elliptical shaped bluff-bodies strategically placed in the zones indicated by the wavemaker is presented.

4.1. Steady State Flow Solution – no control bluff-bodies

The steady state flow equations are solved in FreeFEM++ with the classic Newton method for solving partial derivative equations, which considers an initial value for the flow parameters and iterates the results until a certain residual value is reached [23]. For the current case the minimum residuals are set to 10^{-6} for all flow parameters as it is considered enough by several researchers to prevail relevant results and the simulation converged in about 7 iterations [24]. A recirculation zone indicated by a negative sign of the streamwise velocity is observed behind the circle. In the detail shown in Fig. 3, the flow values are set to a maximum of zero, so the recirculation zone is highlighted. The total recirculation length, L_x, is about ~4.9D. Similar values are also reported in the literature [18].

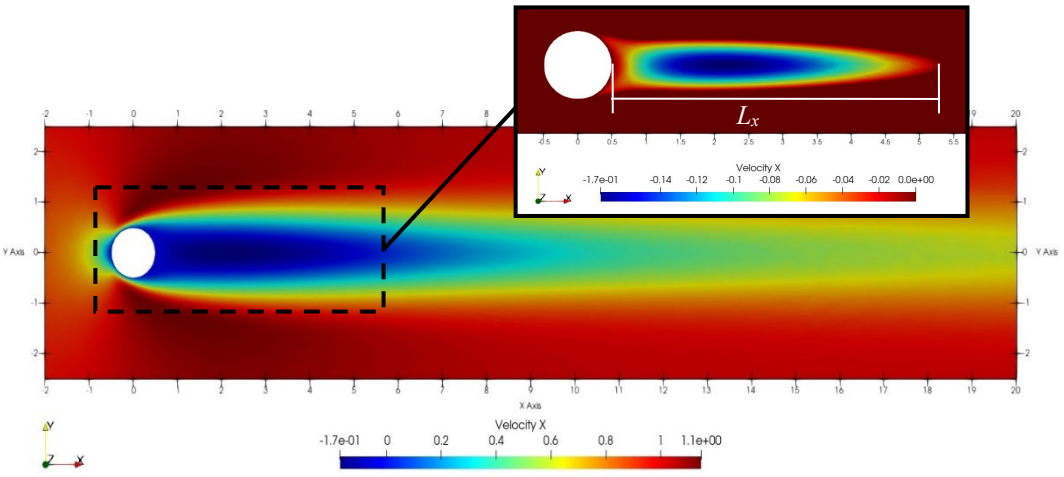

Fig. 3. Streamwise velocity - steady state

4.2. Unsteady State Flow Solution – no control bluff-bodies

The unsteady state simulations are carried out with a time step of $\Delta t = 0.05$ and running for 6000 iterations. A monitoring point (*MP*) is placed at the location $(x, y) = (2.5, 0.5)$ which is slightly off-axis. After ~30 time steps, a transition from a columnar to a slightly oscillating flow is observed. After ~75 time steps, small vortices are observed the wake of the 2D cylinder. At non-dimensional time units The transition to a periodical vortex shedding is completed at ~115 time steps, see Fig. 4.

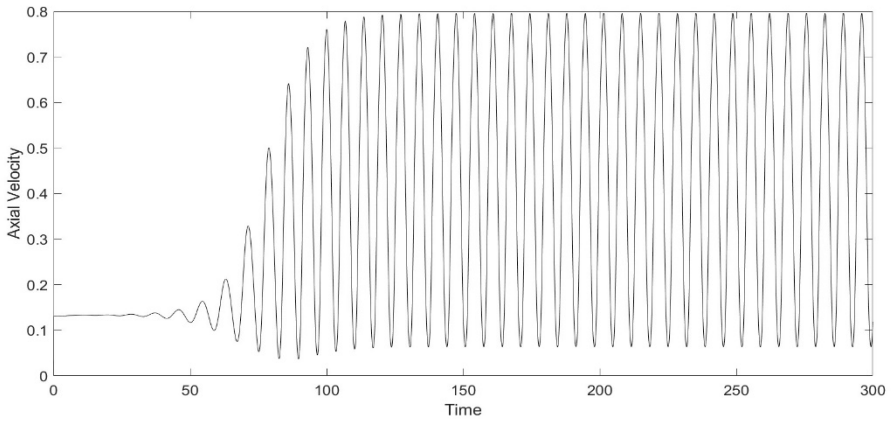

Fig. 4. Streamwise velocity in function of time at *MP(2.5,0.5)*

Using Fig. 4, 20 periods of developed vortex shedding are used to time-average the flow. Also, a Fast Fourier Transform is applied in the same conditions revealing a vortex shedding frequency of *f=0.148*, see Fig. 5.

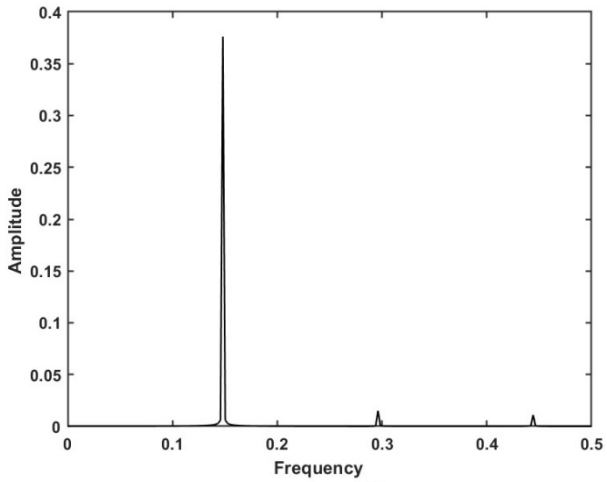

Fig. 5. Vortex shedding frequency at Re = 80

4.3. Linear Global Stability Analysis (Global LSA)

The global LSA is first carried on considering the steady state and the mean flow fields. In each case the spatial structures of the most unstable modes (direct and adjoint) are computed using the procedure detailed in [21]. The leading eigenvalue related to the most unstable mode is used to determine if the flow is linearly stable or unstable based on the growth rate sign. The imaginary part of the eigenvalue returned by the FreeFEM++ software is the angular frequency. Hence all the results shown further must be divided by 2π to obtain the correct values of the characteristic frequencies. The eigenvalue problems are solved using the shift-invert Arnoldi method which require a reference value [23], [25].

4.3.1. Steady state flow

The leading eigenvalue of the global LSA in the steady state flow is found to be $\omega_{steady}=0.093+i0.742$. Similar values are reported in the literature as it is shown in table 1 [15].

Table 1

Global LSA of the steady state flow

	Current paper		Literature [15]	
Re	Growth rate	Frequency	Growth rate	Frequency
80	0.093	0.118	0.096	0.120

The global LSA of the steady state flow cannot handle the nonlinearities of the vortex shedding and it does not succeed to capture the instabilities frequency as it also reported in [15]. The spatial structures that have the most unstable eigenmode are shown in Fig. 6.

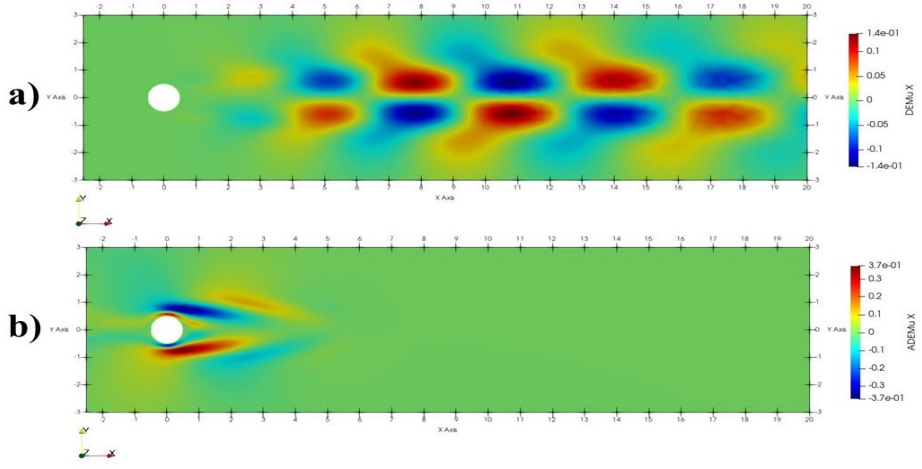

Fig. 6. Real part of the streamwise component for Steady state case: a) Direct eigenmode, and b) Adjoint eigenmode

It is observed that the direct eigenmode develops in the bluff-body wake while the adjoint eigenmode is concentrated in its close vicinity and tends to propagate upstream too. Interpreted separately, the direct and adjoint eigenmodes do not provide relevant data about the onset of the instabilities. Hence, the idea of using the dot product shown in equation (7) is to overlap the spatial structures of the direct and adjoint eigenmodes to obtain the maximum receptive zone to a base flow modification.

4.3.2. Mean unsteady flow

The leading eigenvalue of the global LSA of the mean flow is found to be ω_{mean}=*-0.009+i0.944*. In this case, the dimensionless frequency is found to be ~0.150 which is roughly 1.35% overestimated compared to the vortex shedding frequency from the numerical simulations presented in Section 4.2. The real part of the eigenvalue, representing the growth rate is almost zero, leading to the idea that when the mean flow is associated to a steady solution it is marginally stable [15]. The comparison to the literature results is presented in table 2.

Table 2

Global LSA of the mean flow

	Current paper		Literature [15]	
Re	Growth rate	Frequency	Growth rate	Frequency
80	-0.009	0.15	0	0.155

The spatial structures of the instabilities look similar to the ones from the global LSA of the steady state flow. Still, a difference appears especially in the amplitudes of the results as observed in Fig. 7.

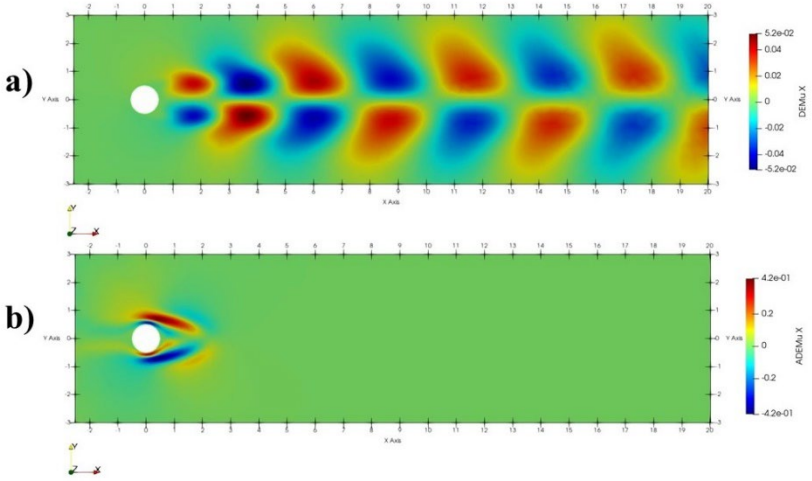

Fig. 7. Real part of the streamwise component for Mean flow case: a) Direct eigenmode, and b) Adjoint eigenmode;

4.3.3. Sensitivity analysis

The sensitivity map shown in Fig. 8 reveals the regions where the flow presents the maximum receptivity to a force that can be applied to attenuate the instabilities.

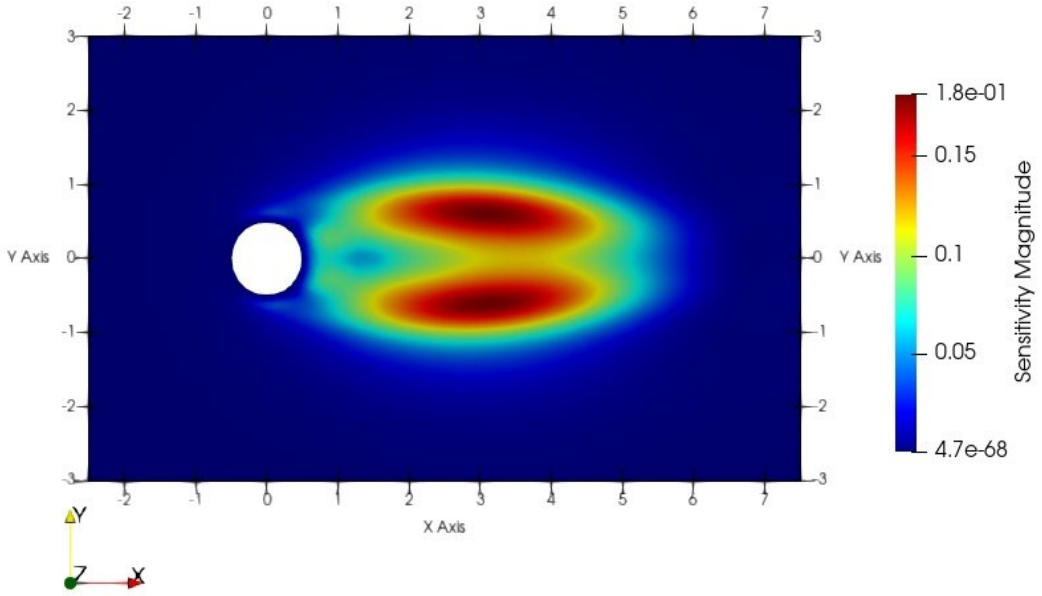

Fig. 8. Sensitivity map based on the steady state flow

Two symmetrical lobes are observed in Fig. 8 in the wake of the circle close to the recirculation zone. Outside of the two lobes area the sensitivity amplitude is almost zero. Hence, the direct and adjoint global LSA represents a powerful tool on understanding the dynamics of the instabilities when they are studied together instead of being analyzed separately. Similar sensitivity maps are presented in the literature [18].

4.3.4. Control based on the Steady state flow

Once the most powerful feedback zones are determined, an external force may be inserted into the governing equations to modify the flow dynamics and implicitly stabilize it. In the current paper the flow dynamics are modified by inserting different bluff-bodies in the wake of the region. Firstly, two small circles of a diameter d=0.1D are physically modelled at the locations: (x_{c1},y_{c1}=3.1,0.5), respectively (x_{c2},y_{c2}=3.1,-0.5). Secondly, two elliptical shapes are placed with their centre in the same locations. The elliptical shapes present an aspect-ratio of the major-to-minor axis of 3, where the major axis has a length of 3D and the minor axis has a length of 1D.

The exact positions of the bluff-bodies are illustrated in Fig. 9 a) and b) for the small control circles, respectively the elliptical shaped ones.

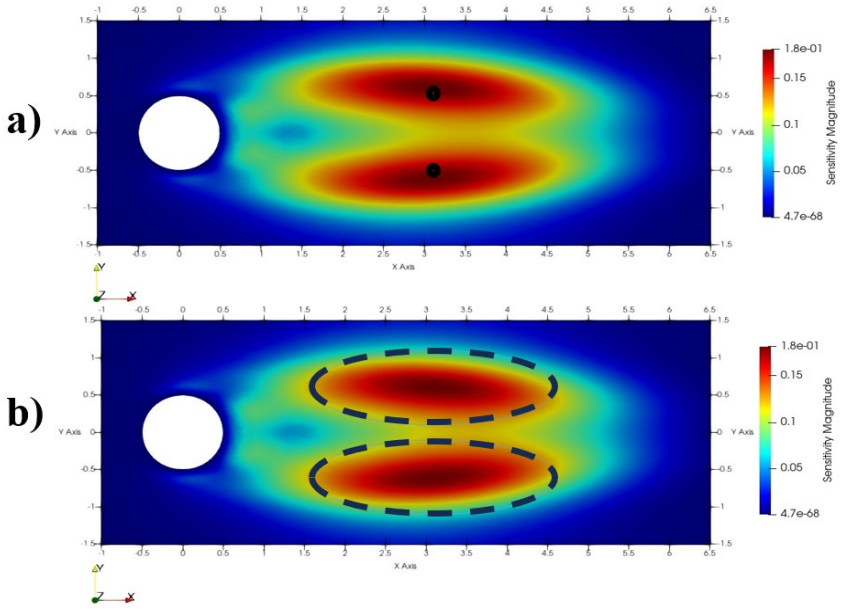

Fig. 9. Control bluff-bodies positions

As mentioned earlier, the eigenvalue problems are calculated using the shift-invert Arnoldi methods [25], [26]. This method requires a reference value for the eigenvalue so the solver seeks and returns the closest results at a given margin of error. Therefore, the leading eigenvalue being unknown in these cases, the most unstable eigenvalue from the previous case is used as a reference (see Section 4.3.1).

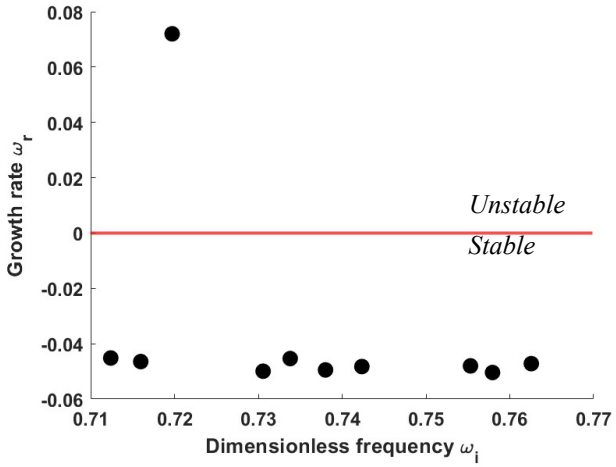

Fig. 10. Eigenvalues spectrum – two small control circles

The global LSA of the steady flow with two small control circles reveals a leading eigenvalue of $\omega_{cc}=0.072+i0.72$. The placement of two small control circles manages to decrease the most unstable eigenmode growth rate by ~29.17%.

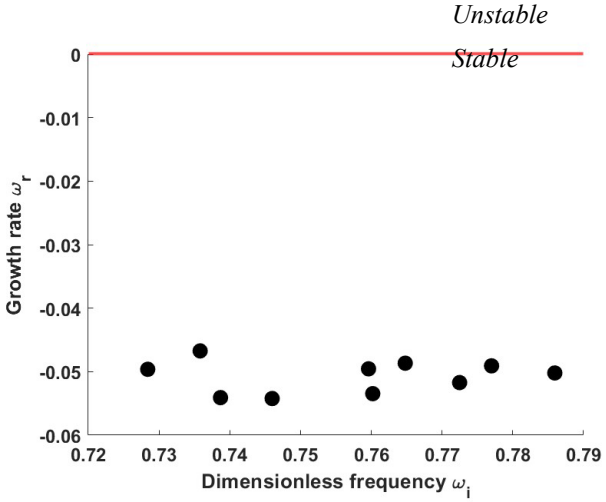

Fig. 11. Eigenvalues spectrum – two control elliptical bodies

Moreover, the global LSA around the steady flow with two elliptical shapes in the wake of the circle returns only eigenvalues with negative growth rates, hence the flow is linearly stabilized.

5. Conclusions

The vortex shedding dynamics behind bluff-body of circular shape at Re = 80 are analyzed through a global LSA. Firstly, the steady state, i.e., time-independent, solution is obtained with the Newton iterative method. The results are validated with the available data in the literature using one of the most studied quantities of the flow around a circle, the recirculation length. The recirculation length is found to be ~4.9*D* as it is reported in [18]. The flow field from the steady state solution is considered as the initial condition for the unsteady case, i.e., the time dependent solution. A monitoring point is added in the circle wake just off-axis to acquire the axial velocity at each time step. The transition to a slightly oscillating flow is observed after ~30 non-dimensional time units. Small vortices are observed to burst in the wake of the circle after ~75 non-dimensional time units. The transition to the vortex shedding is completed and becomes periodical after ~115 non-dimensional time units. An interval of 20 fully developed cycles of vortex shedding is used to time average the flow. A Fast Fourier Transform (FFT) is performed on the same interval. The vortex shedding frequency is found to be $f = 0.148$.

The global LSA of the steady state flow reveals a leading unstable eigenvalue $\omega_{steady}=0.093+i0.742$ compared to $\omega_{steadyLiterature}=0.096+i0.754$ reported in literature [15]. The imaginary parts represent an angular frequency which must be divided by 2π to get the dimensionless frequency. Thus, the frequency of the instability is approximately 0.118, while a frequency of 0.12 is reported in [15]. In

both cases it is observed that the frequency of the instability is underestimated compared to the vortex shedding frequency. It is concluded that the global LSA of the steady flow cannot handle the nonlinearities of the vortex shedding and it fails to predict the frequency of the instability.

The global LSA of the mean flow reveals a leading unstable eigenvalue ω_{mean}=*-0.009+i0.944*. While the dimensionless frequency is found to be ~0.150 which is roughly 3.22% underestimated compared to the literature, the growth rate is close to 0. In this case, when the mean flow is used as a steady solution for the global LSA, it is marginally stable.

The sensitivity analysis of the steady flow reveals two axisymmetric lobes in the wake of the circle. Firstly, two small control circles with a diameter of d=0.1D each are placed in the most receptive zones indicated by the lobes. The global LSA of the steady flow with two small control circle reveals that the most unstable mode growth rate is reduced by ~29.17%. Secondly, two elliptical shaped bluff-bodies are places with their center in the same positions indicated by the sensitivity analysis. The global LSA of the steady flow with elliptical bluff-bodies returns only eigenvalues with negative signs meaning that the flow is linearly stable.

The passive control technique with different bluff-bodies is used in a simple flow configuration to determine the influence on the flow dynamics and its stability. These techniques can be further developed and used in more complex geometries such as the flow inside the hydraulic turbines to stabilize the flow and extend the operational domain of these machines at a maximum efficiency with minimal cavitation.

Acknowledgment

The results presented in this article have been funded by the Ministry of Investments and European Projects through the Human Capital Sectoral Operational Program 2014-2020, Contract no. 62461/03.06.2022, SMIS code 153735. This work was also supported by a grant of the Ministry of Research, Innovation and Digitization, CCCDI - UEFISCDI, project number PN-III-P2-2.1-PTE-2021-0269, within PNCDI III.

REFERENCES

[1]. European Commission, “European policy: Climate strategies and targets”, 2017

[2]. *S. Pasche*, “Dynamics and Optimal Control of Self-Sustained Instabilities in Laminar and Turbulent Swirling Flows: Application to the Part Load Vortex Rope in Francis Turbines”, PhD Thesis, École Polytechnique Fédérale de Lausanne, Lausanne, Switzerland, 2018

[3]. *M. Kurosaka, M. Kikuchi, K. Hirano, T. Yuge, H. Inoue*, “Interchangeability of vortex-breakdown types”, in Experiments in Fluids, **vol. 34**, pp. 77-86, 2003

[4]. *R. Resiga, S. Muntean, V. Hasmatuchi, I. Anton, F. Avellan*, “Analysis and Prevention of Vortex Breakdown in the Simplified Discharge Cone of a Francis Turbine”, in Journal of Fluids Engineering, **vol. 132**, 2010

[5]. *I.S. Grecu, G. Dunca, D.M. Bucur and M.J. Cervantes*, “URANS numerical simulations of pulsating flows considering streamwise pressure gradient on asymmetric diffuser”, in IOP Conf. Ser: Earth Environ. Sci.1079, 2022

[6]. *D. H. Peckham and S. A. Atkinson*, “Preliminary results of flow speed wind tunnel tests on a gothic wing of aspect ratio1.0,” Aeronautical Research Council Current Paper No. 508, 1957.

[7]. *T. Sarpkaya*, "On stationary and travelling vortex breakdowns," Journal of Fluid Mechanics, **vol. 45**, no. 3, pp. 545–559, Feb. 1971, doi: https://doi.org/10.1017/s0022112071000181.
[8]. *S. Wang and Z. Rusak*, "The dynamics of a swirling flow in a pipe and transition to axisymmetric vortex breakdown," Journal of Fluid Mechanics, **vol. 340**, pp. 177–223, Jun. 1997, doi: https://doi.org/10.1017/s0022112097005272.
[9]. *F. Bunea, G. D. Ciocan, D. M. Bucur, G. Dunca, and A. Nedelcu*, "Hydraulic Turbine Performance Assessment with Implementation of an Innovative Aeration System," Water, **vol. 13**, no. 18, pp. 2459–2459, Sep. 2021, doi: https://doi.org/10.3390/w13182459.
[10]. *M. Nishi, X. M. Wang, K. Yoshida, T. Takahashi, and T. Tsukamoto*, "An Experimental Study on Fins, Their Role in Control of the Draft Tube Surging," in Hydraulic Machinery and Cavitation, Netherlands: Dordrecht: Springer , 1996, pp. 905–914.
[11]. *R. Susan-Resiga, T. C. Vu, S. Muntean, G. D. Ciocan, and B. Nennemann*, "Jet control of the draft tube vortex rope in Francis turbines at partial discharge," in Proceedings of the 23th IAHR Symposium on Hydraulic Machinery and Systems, Yokohama, Japan, 2006.
[12]. *R. F. Susan-Resiga, S. Muntean, F. Avellan, and I. Anton*, "Mathematical modelling of swirling flow in hydraulic turbines for the full operating range," Applied Mathematical Modelling, **vol. 35**, no. 10, pp. 4759–4773, Oct. 2011, doi: https://doi.org/10.1016/j.apm.2011.03.052.
[13]. *O. Reynolds*, "An experimental investigation of the circumstances which determine whether the motion of water shall be direct or sinuous and of the law of resistance in parallel channels," in Phil. Trans. Roy. Soc., 1883.
[14]. *V. Theofilis*, "Advances in global linear instability analysis of nonparallel and three-dimensional flows, Progress in Aerospace Sciences, **vol. 39**, issue 4, pp. 249-315, 2003
[15]. *D. Barkley*, "Linear analysis of the cylinder wake mean flow", in Europhysics Letters, **vol. 75**, no. 5, 2006
[16]. *S. Pasche, François Gallaire, and F. Avellan*, "Predictive control of spiral vortex breakdown," Journal of Fluid Mechanics, **vol. 842**, pp. 58–86, May 2018, doi: https://doi.org/10.1017/jfm.2018.124.
[17]. *P. J. Strykowski and K. R. Sreenivasan*, "On the formation and suppression of vortex 'shedding' at low Reynolds numbers," Journal of Fluid Mechanics, **vol. 218**, p. 71, Sep. 1990, doi: https://doi.org/10.1017/s0022112090000933.
[18]. *F. Giannetti, P. Luchini*, "Structural sensitivity of the first instability of the cylinder wake", in Journal of Fluid Mechanics, **vol. 581**, pp. 167-197, 2006
[19]. *O. Marquet, D. Sipp, and L. Jacquin*, "Sensitivity analysis and passive control of cylinder flow," Journal of Fluid Mechanics, **vol. 615**, pp. 221–252, Nov. 2008, doi: https://doi.org/10.1017/s0022112008003662.
[20]. *Z. Seifi, M. Raisee, M. J. Cervantes*, "Global linear stability analysis of flow inside an axial swirl generator with a rotating vortex rope" in Journal of Hydraulic Research, **vol. 61**, no. 1, pp. 34-50, 2023
[21]. *R. Mitrut, D.M. Bucur, G. Dunca, M.J. Cervantes*, "Linear Global Stability Analysis of a Laminar Flow Around a Circular Body", in 12th International Symposium on Advanced Topics in Electrical Engineering, 2021
[22]. *F. Giannetti, S. Camarri, V. Citro*, "Sensitivity analysis and passive control of the secondary instability in the wake of a cylinder", in Journal of Fluid Mechanics, **vol. 864**, pp. 45-72, 2019
[23]. *F. Hecht*, "New development in freefem++" in Journal of Numerical Mathematics, **vol. 20**, no. 3-4, pp. 251-265, 2012
[24] *R. Goyal* Flow, "Field in a High Head Francise Turbine Draft Tube During Transient Operations", PhD Thesis, Luleå University of Technology, Sweden , 2018
[25]. *W. E. Arnoldi*, "The Principle of Minimized Iterations in the Solution of the Matrix Eigenvalue Problem," Quarterly of Applied Mathematics, **vol. 9**, no. 1, pp. 17–29, 1951
[26]. *D. Fabre, V. Citro, D. Ferreira Sabino, P. Bonnefis, J. Sierra, F. Giannetti, M. Pigou*, "A Practical Review on Linear and Nonlinear Global Approaches to Flow Instabilities", in Applied Mechanics Review, **vol 70**, no. 6, 2018